

Limit cycles can reduce the width of the habitable zone

Jacob Haqq-Misra^{1,2}, Ravi Kumar Kopparapu^{1,2,3,4}, Natasha E. Batalha^{2,5,6}, Chester E. Harman^{2,6,7}, and James F. Kasting^{2,6,7}

ABSTRACT

The liquid water habitable zone (HZ) describes the orbital distance at which a terrestrial planet can maintain above-freezing conditions through regulation by the carbonate-silicate cycle. Recent calculations have suggested that planets in the outer regions of the habitable zone cannot maintain stable, warm climates, but rather should oscillate between long, globally glaciated states and shorter periods of climatic warmth. Such conditions, similar to ‘Snowball Earth’ episodes experienced on Earth, would be inimical to the development of complex land life, including intelligent life. Here, we build upon previous studies with an updated an energy balance climate model to calculate this ‘limit cycle’ region of the habitable zone where such cycling would occur. We argue that an abiotic Earth would have a greater CO₂ partial pressure than today because plants and other biota help to enhance the storage of CO₂ in soil. When we tune our abiotic model accordingly, we find that limit cycles can occur but that previous calculations have overestimated their importance. For G stars like the Sun, limit cycles occur only for planets with CO₂ outgassing rates less than that on modern Earth. For K and M star planets, limit cycles should not occur; however, M-star planets may be inhospitable to life for other reasons. Planets orbiting late G-type and early K-type stars retain the greatest potential for maintaining warm, stable

¹Blue Marble Space Institute of Science, 1001 4th Ave Suite 3201, Seattle, WA 98154, USA

²NASA Astrobiology Institute’s Virtual Planetary Laboratory, P.O. Box 351580, Seattle, WA 98195, USA

³NASA Goddard Space Flight Center, 8800 Greenbelt Road, Mail Stop 699.0 Building 34, Greenbelt, MD 20771, USA

⁴Department of Astronomy, University of Maryland, College Park, MD 20742, USA

⁵Department of Astronomy and Astrophysics, The Pennsylvania State University, University Park, PA 16802, USA

⁶Center for Exoplanets and Habitable Worlds, The Pennsylvania State University, University Park, PA 16802, USA

⁷Department of Geosciences, The Pennsylvania State University, University Park, PA 16802, USA

conditions. Our results suggest that host star type, planetary volcanic activity, and seafloor weathering are all important factors in determining whether planets will be prone to limit cycling.

Subject headings: planetary habitability, astrobiology, climate modeling, complex life, Rare Earth hypothesis

1. Introduction

Earth’s orbit falls within the boundaries of the habitable zone (HZ) where a rocky planet can maintain liquid water on its surface, given a $\text{CO}_2\text{-N}_2\text{-H}_2\text{O}$ atmosphere and some mechanism (e.g., plate tectonics) for recycling these volatiles (Kasting et al. 1993; Abe et al. 2011; Kopparapu et al. 2013, 2014; Leconte et al. 2013; Wolf & Toon 2014; Yang et al. 2014). The inner HZ edge is bounded by either the runaway greenhouse effect, in which liquid water evaporates entirely, or the moist greenhouse¹ effect, in which liquid water persists on a planet’s surface but the stratosphere becomes wet and water is lost by photodissociation followed by escape of hydrogen to space. The moist greenhouse effect is difficult to simulate with one-dimensional models that assume a saturated troposphere (Kopparapu et al. 2013), but it does appear in some general circulation models (Wolf & Toon 2014). Planets farther out in the HZ are expected to accumulate dense CO_2 atmospheres because of the negative feedback between silicate weathering (the loss process for atmospheric CO_2) and surface temperature (Walker et al. 1981). But this feedback loop is ultimately limited by CO_2 condensation and Rayleigh scattering, which combine to create an outer HZ boundary termed the ‘maximum greenhouse limit’ (Kasting et al. 1993). A proposed extension of the outer HZ boundary by formation of CO_2 ice clouds (Forget & Pierrehumbert 1997; Mischna et al. 2000; Colaprete & Toon 2003; Forget et al. 2013) appears less likely when the ‘scattering greenhouse effect’ of these clouds is recomputed using more accurate radiative transfer models, (Kitzmann 2016).

The conventional thinking regarding the HZ outer edge may be too optimistic, however, because it fails to account for mass transfer rates of CO_2 . CO_2 is released from volcanoes and is consumed by silicate weathering followed by deposition of carbonate sediments (Walker et al. 1981; Berner et al. 1983). These processes are in approximate balance on

¹We use the term ‘moist greenhouse’ throughout our paper, although we acknowledge that this may be imprecise terminology, as Earths present atmosphere could be described as a moist greenhouse. Other terms such as ‘moist stratosphere’ or ‘diffuse tropopause’ might be better descriptors of this phenomenon, but they suffer from sounding arcane or obscure.

modern Earth, creating a climate that is stable and relatively warm, even if it is sometimes perturbed by glacial-interglacial cycles. Occasional ‘Snowball Earth’ episodes in which the planet is fully glaciated (Hoffman et al. 1998) have been attributed to a variety of complicating factors, including changes in atmospheric O_2 and CH_4 (Pavlov et al. 2003), as well as limit cycles involving atmospheric CO_2 (Tajika 2007; Mills et al. 2011). Limit cycles—oscillations between ice-free and globally glaciated states—occur in models of the early Earth in which volcanic outgassing rates are too low to sustain a CO_2 -warmed climate (Tajika 2007).

Several new papers have argued that such limit cycle behavior could be far more prevalent than previously thought (Kadoya & Tajika 2014, 2015; Menou 2015). Depending on the volcanic outgassing rate and host stellar type, some Earth-like planets are subject to climatic limit cycles when stellar insolation is low, as it is in the outer parts of a star’s HZ. All of these recent studies employed parameterized versions of energy-balance climate models (EBMs). Such models include radiative balance between incident stellar and outgoing infrared radiation, along with diffusional heat fluxes between different latitude bands. These models are useful tools for studying climate variations that occur on time scales of thousands to tens of millions of years.

Here we discuss the possibility that limit cycles could reduce the outer edge of the HZ. We use our own EBM, which implements an updated parameterization of radiative transfer based on 1-D radiative-convective HZ calculations (Kopparapu et al. 2013, 2014). Our model includes a representation of the carbonate-silicate cycle used by previous studies (Menou 2015), and also expands on previous work to include the effect of CO_2 condensation and the impact of seafloor weathering. These improvements allow us to determine, for the first time, the limit cycle boundaries relative to the conventional liquid water HZ for different types of stars.

2. Model Description

Latitudinal energy balance models (EBMs) are computationally efficient models that are well-suited to exploring glacial cycling and its influence on climate. Although EBMs can be useful with a highly idealized linearization of infrared absorption (North et al. 1981; Gaidos & Williams 2004; Haqq-Misra 2014), investigation of HZ limits requires an EBM with a more sophisticated radiative transfer parameterization (Williams & Kasting 1997; Fairén et al. 2012; Vladilo et al. 2013; Kadoya & Tajika 2014; Menou 2015). However, no previously published EBM has yet been updated to include parameterizations based upon radiative-convective HZ model calculations (Kopparapu et al. 2013, 2014), which use coefficients derived from the HITRAN 2008 (Rothman et al. 2009) and HITEMP 2010 (Rothman et al.

2010) spectroscopic databases to account for additional absorption features of H₂O and CO₂ compared to earlier models (Kasting et al. 1993). Existing EBMs that consider planetary habitability (Vladilo et al. 2013; Kadoya & Tajika 2014, 2015; Menou 2015) use an older radiation scheme (Williams & Kasting 1997), which is based upon a polynomial parameterization of prior radiative-convective calculations (Kasting 1991). These EBM investigations continue to be useful for interpreting exoplanet habitability and guiding more complicated modeling studies toward interesting regions of parameter space, but the lack of up-to-date radiative transfer parameterization in such models can limit their utility when comparing with other recent climate models or interpreting exoplanet observations.

We use a one-dimensional EBM that has been developed in previous studies (Williams & Kasting 1997; Gaidos & Williams 2004; Fairén et al. 2012; Haqq-Misra 2014). This EBM calculates meridionally averaged temperature T as a function of latitude θ and time t according to the equation

$$C \frac{\partial T}{\partial t} = \bar{S} (1 - \alpha) - F_{OLR} + \frac{1}{\cos \theta} \frac{\partial}{\partial \theta} \left(D \cos \theta \frac{\partial T}{\partial \theta} \right). \quad (1)$$

Eq. (1) expresses the change in temperature as the sum of stellar heating, infrared cooling, and meridional diffusion. Diurnally averaged solar flux $\bar{S} = S \cdot q(\theta)$ is the product of a constant solar flux S and a function of latitude $q(\theta)$ (which assumes a circular orbit) to yield seasonally varying insolation (Gaidos & Williams 2004). The effective heat capacity of the surface and atmosphere, C , depends on the fraction of ocean and ice coverage at a given latitude (Williams & Kasting 1997; Fairén et al. 2012). We prescribe Earth-like conditions by setting 70% ocean coverage at all latitudes and allowing fractional ice coverage between 263 K to 273 K. Radiative fluxes are represented by the top-of-atmosphere albedo α and the infrared outgoing radiative flux F_{OLR} . Our FORTRAN implementation of this EBM is discretized into 18 equally spaced latitudinal zones with a initial uniform temperature profile of $T = 233$ K and stepped through 1000 (or more) complete orbits by increments of $\Delta t = 8.64 \times 10^3$ s to numerically solve Eq. (1) with a forward finite differencing scheme². We initialize all simulations with snowball conditions ($T = 233$ K) and CO₂ partial pressure $p\text{CO}_2 = 3.3 \times 10^{-4}$ bar.

The diffusive parameter, D , describes the efficiency of meridional energy transport and scales with changes in atmospheric pressure, heat capacity, atmospheric mass, and rotation

²We can be confident that our choice of parameters will yield a converged solution by examining the CFL condition for numerical stability, $C \leq C_{max}$, where $C_{max} = 1$ for explicit time-marching solvers like ours. If we approximate our length interval as the radius of Earth divided by the total number of latitudinal bands, and if we assume a typical advective wind speed on Earth of $u = 10 \text{ m s}^{-1}$, then $C = u\Delta t/\Delta x = 0.24 < C_{max}$. Only when the number of latitude bands approaches ~ 75 does $C \approx C_{max}$.

rate (Williams & Kasting 1997). This parameter accounts for the exchange of sensible and latent energy fluxes between the tropics and midlatitudes by adjusting the energy balance equilibrium temperature at each latitude. Williams & Kasting (1997) assumed that D is proportional to the inverse square of rotation rate, so that a more rapidly (slowly) rotating planet will show a decreased (increased) tendency toward meridional energy distribution. This behavior mimics well-known results from general circulation models (Williams & Hallway 1982; Showman et al. 2013) while still maintaining the computational efficiency of an EBM. We focus our study on a model planet with a rotation rate equal to present-day Earth, but this assumption does not significantly alter our results. A more slowly rotating planet would have increased meridional energy transport and would therefore tend toward uniform conditions at all latitudes; such a limit is analogous to the globally-averaged EBM used by Menou (2015). A more rapidly rotating planet would show more extreme variations between equatorial and polar temperatures, but this contrast does not significantly alter the onset of global glaciation and deglaciation events. Sensitivity studies indicate that either of these cases will still exhibit transitions into a limit cycle state at approximately the same value of solar constant, so our assumption of a fixed present-day rotation rate does not necessarily limit the scope of our calculations.

Surface albedo a_s is calculated as a weighted sum of the albedos of unfrozen land, unfrozen ocean, and ice coverage at each latitude. We assume an albedo of 0.2 for unfrozen land, while the albedo of ocean varies as a function of solar zenith angle (Williams & Kasting 1997; Fairén et al. 2012). We also implement a band-dependent ice albedo (Pollard & Kasting 2005) that partitions the broadband ice albedo a_i into a visible component, $a_{i,vis} = 0.8$, and a near-infrared component, $a_{i,nir} = 0.5$. This latter value applies to snow-covered ice, as we discuss further below. According to Shields et al. (2013), the near-IR albedo of bare ice is ~ 0.3 . Our model does not include a hydrologic cycle, and so it does not calculate the ratio of bare ice to snow-covered ice, as previous studies (Shields et al. 2013) did. For a given stellar spectrum, we define total ice albedo as the sum $a_i = a_{i,vis}f_{vis} + a_{i,nir}f_{nir}$, where f_{vis} and f_{nir} are the respective percent contributions of visible (≤ 700 nm) and near-infrared (> 700 nm) radiation. Following a previously published method (Kopparapu et al. 2013, 2014), we use BT-Settl model spectra (Allard et al. 2007) to calculate the percent contribution of visible and near-infrared radiation for F-type (7200 K, 67% visible), G-type (5800 K, 52% visible), K-type (4600 K, 32% visible), and M-type (3400 K, 10% visible) stars.

We parameterize the infrared outgoing radiative flux F_{OLR} as a fourth-order polynomial function of the partial pressure of carbon dioxide, $p\text{CO}_2$, and surface temperature, T . Likewise, we parameterize top-of-atmosphere albedo α as a third-order polynomial function dependent on $p\text{CO}_2$, T , surface albedo a_s , and stellar zenith angle. Assuming a noncondensable background pressure of 1 bar N_2 , we use a radiative-convective climate model developed

for HZ calculations (Kopparapu et al. 2013, 2014) to obtain best fits of more than 50,000 calculations for F_{OLR} and α over a parameter space spanning 10^{-5} bar $< p\text{CO}_2 < 35$ bar, 150 K $< T < 350$ K, and $0.2 < a_s < 1$, across all zenith angles. We calculate separate radiative transfer parameterizations for F, G, K, and M stars, using model spectra (Allard et al. 2007), which we describe further in the Appendix.

We assume in our EBM that any condensing CO_2 accumulates on the surface as dry ice. CO_2 condensation occurs when $p\text{CO}_2$ exceeds the CO_2 saturation vapor pressure at surface temperature T within a latitudinal zone. We assume that dry ice will radiatively dominate over water ice, so we set total ice albedo $a_i = 0.35$ for frozen carbon dioxide (Warren et al. 1990) when CO_2 condensation occurs. We also keep an inventory of the thickness of CO_2 ice that condenses or melts on the surface at a given latitude, and we adjust the radiative contribution of CO_2 at each latitude, as well as the global value of $p\text{CO}_2$, by a corresponding amount each iteration. We calculate the thickness z of accumulating ice as $z = \Delta(p\text{CO}_2)/g\rho$, where $\Delta(p\text{CO}_2)$ is the partial pressure of CO_2 that condenses into ice, $g = 9.81$ m s $^{-2}$, and $\rho = 1600$ kg m 3 is the density of dry ice. Assuming that ice thickness is limited only by geothermal heat flow, we express the maximum CO_2 ice thickness as: $z_{max} = k\Delta T/F_g$ (Pollard & Kasting 2005), where $k = 0.6$ W m $^{-1}$ K $^{-1}$ is the thermal conductivity of solid CO_2 (Kravchenko & Krupskii 1986; Stewart & Nimmo 2002), ΔT is the temperature difference between the atmosphere and seawater beneath the ice, and $F_g = 0.1$ W m $^{-2}$ is an Earth-like geothermal heat flux. For a temperature difference $\Delta T = 25$ K characteristic of a globally glaciated planet (Pollard & Kasting 2005), this gives a maximum CO_2 ice thickness of $z_{max} = 150$ m. Any additional accumulation would result in basal melting of CO_2 glaciers and the transport of liquid CO_2 to lower latitudes, although none of our simulations in this study reach conditions where $z > z_{max}$.

Our latitudinal model can only represent clouds through adjustments to surface albedo, and we assume in our calculations that water clouds cover half of the surface. We have explored the sensitivity of climate to this cloud fraction parameter in a previous study (Fairén et al. 2012), which showed that excessive cloud cover can cause a planet to plummet into global glaciation. We account for the absorption of infrared radiation by clouds by subtracting a fixed amount of 8.5 W m $^{-2}$ from F_{OLR} at each latitude band, following Williams & Kasting (1997). This value was selected by requiring that the EBM should produce a present-day Earth temperature of 288 K when the model is initialized with above-freezing initial conditions at $S/S_0 = 1.0$. Possible sources of additional warming include CO_2 ice clouds, which could warm the surface by up to 15 K by providing additional downward-directed infrared radiation through a scattering greenhouse effect (Forget & Pierrehumbert 1997; Mischna et al. 2000; Colaprete & Toon 2003; Forget et al. 2013). But this is not by itself enough to deglaciate a planet (Forget et al. 2013), and Kitzmann (2016) has shown that

these previous calculations may have significantly overestimated the warming from such clouds. By neglecting their radiative impact, we generate a somewhat pessimistic outer limit on planetary habitability.

2.1. Outgassing Rates

CO₂ accumulates in our model atmosphere as a result of the carbonate-silicate cycle, which allows a frozen planet to eventually deglaciate. We represent the ~ 0.5 Myr timescale of the carbonate-silicate cycle with the time variable, τ , to contrast this slower timescale from the faster time step, t , used in Eq. (1). Following Menou (2015) we implement the time evolution of $p\text{CO}_2$ into our EBM according to

$$\frac{d}{d\tau}(p\text{CO}_2) = V - W - W_{sea}, \quad (2)$$

where V represents the volcanic outgassing rate of CO₂, W represents the uptake of CO₂ by rock weathering, and W_{sea} represents the uptake of CO₂ by seafloor weathering. We begin by assuming volcanic outgassing to be a constant $V = V_{\oplus}$, where V_{\oplus} is the present-day value.

We also re-examine prior assumptions regarding the total rate of CO₂ outgassing. Menou (2015) assumed a value of $V_{\oplus} = 7$ bar/Gyr, which, converted to geochemists' units for an Earth-mass planet, corresponds to rate of $V_{\oplus} = 0.83$ Tmol/yr. Menou (2015) appears to have obtained this value from Abe et al. (2011), who in turn obtained this value from Sasal et al. (2002) as the expected CO₂ flux from the depleted mantle alone. However, best estimates of the total terrestrial CO₂ outgassing rate suggest $V_{\oplus} \approx 7.5$ Tmol/yr (Gerlach 2011; Jarrard 2003), which is about a factor of ten greater than the value used by Menou (2015). By comparison, Tajika (2007) assumed a modern outgassing rate of 8 Tmol/yr. We argue that this modern rate is the best choice for assessing the habitability of a planet with Earth-like tectonic activity. We use a value of $V_{\oplus} = 70$ bar/Gyr in most of our calculations, but we also explore the dependence of V on defining the limit cycle HZ boundary.

2.2. Weathering Rates

The weathering rate in our model includes both land and seafloor processes. For abiotic conditions, Menou (2015) adopted a functional form of W as (Berner & Kothavala 2001)

$$\frac{W}{W_{\oplus}} = \left(\frac{p\text{CO}_2}{p_{\oplus}}\right)^{\beta} e^{k_{act}(T-288)} [1 + k_{run}(T - 288)]^{0.65}, \quad (3)$$

where $W = W_{\oplus} \equiv V_{\oplus}$ for $T_{surf} = 288$ K, $k_{act} = 0.09$ is an activation energy, and $k_{run} = 0.045$ is a runoff efficiency factor. The value of β is a critical factor determining the rate of $p\text{CO}_2$ evolution and has been estimated to be in the range of 0.25 to 1.0 in the absence of vascular plants (Kump et al. 2000; Berner & Kothavala 2001; Abbot et al. 2012). A lower value of $\beta = 0.25$ is appropriate for environmental conditions with $\text{pH} < 5$, and probably represents a minimum dependence of weathering rate on $p\text{CO}_2$ (Berner 1992). Tajika (2007) assumed $\beta = 0.3$, following Walker et al. (1981). Their parameterization, in turn, was based on laboratory studies of silicate dissolution by Lagache (1976). It remains unclear whether or not the presence of widespread biological systems should affect β , although the presence of life should increase the weathering rate W (Cawley et al. 1969; Schwartzman & Volk 1989; Berner 1992). We use a value of $\beta = 0.5$ for most of our calculations, which is appropriate for conditions under which the weathering rate is proportional to dissolved $[\text{H}^+]$. We also perform a more limited set of calculations for $\beta = 0.3$.

Seafloor weathering has been neglected in previous calculations of limit cycling, but that is probably an oversight, particularly for planets with smaller amounts of land area than Earth. We consider the effects of seafloor weathering by assuming that the seafloor weathering rate is independent of temperature according to the functional form

$$W_{sea} = W_s \left(\frac{p\text{CO}_2}{p_{\oplus}} \right)^{\gamma}, \quad (4)$$

where γ is a seafloor weathering parameter analogous to β in Eq. (3) and W_s is the base-line seafloor weathering that occurs in the absence of any $p\text{CO}_2$ dependence. Increases in the value of W_{sea} or γ cause a reduction in the frequency of limit cycling until a state of permanent glaciation occurs. This parameter γ may be near unity, but weaker weathering dependence with $\gamma = 0.4$ or lower may also be consistent with some computed histories of early Earth (Sleep & Zahnle 2001). We initially assume $W_s = 0$ in our calculations to assess the limit cycle boundary of the HZ, and we then consider sensitivity to changes in the seafloor weathering rate.

2.3. Partial pressure of CO_2 in soil

A critical factor in determining the onset of limit cycles in the HZ is the partial pressure of CO_2 in soil. The parameter p_{\oplus} represents the long-term balance between atmospheric and soil CO_2 for present-day Earth. Menou (2015) assumed a value of $p_{\oplus} = 3.3 \times 10^{-4}$ bar to represent the pre-industrial CO_2 level. However, the long-term balance between weathering and volcanism should be based on the value of $p\text{CO}_2$ in soil, rather than in the atmosphere. This implies that an abiotic Earth should have a higher value of atmospheric $p\text{CO}_2$ than

today. To put it another way, if all of life were to suddenly vanish, then $p\text{CO}_2$ should increase until the atmospheric and soil (regolith) partial pressures were equal. If we wish to use our model to test the habitability of abiotic planets, or of inhabited planets that lack vascular land plants, then we should tune the model to an abiotic state.

For a biotic planet like present-day Earth, root respiration by vascular plants increases the value of soil $p\text{CO}_2$ by a factor of 10 to 100 (Kump et al. 2010). We assume here that the enhancement is a factor of 30, in which case soil $p\text{CO}_2$ should be approximately 10^{-2} bar. For $\beta = 0.5$, this implies that land plants accelerate silicate weathering by a factor of $30^{0.5} \approx 5.5$. For $\beta = 0.3$, the acceleration would be $30^{0.3} \approx 2.8$. In either case, an abiotic present-day Earth would be warmer than today because land plants would no longer be pumping atmospheric CO_2 into soil. We therefore choose a value of $p_{\oplus} = 10^{-2}$ bar for our calculations of the limit cycle HZ boundary.

3. Results

We first consider an Earth-like (but abiotic) planet orbiting a G-type star like the Sun. At present-day stellar flux ($S/S_0 = 1.0$), our weathering model for abiotic Earth with $\beta = 0.5$ balances at soil $p\text{CO}_2 = 1.8 \times 10^{-3}$ bar and average surface temperature of 296 K, while present Earth (with life) at a temperature of 288 K has a higher value of soil $p\text{CO}_2 = 10^{-2}$ bar (Fig. 1). By contrast, Menou (2015) argued that the carbon cycle on an abiotic Earth should balance at 288 K and $p\text{CO}_2 = 3.3 \times 10^{-4}$ bar. This would only be true if land plants had zero effect on silicate weathering. Our model agrees with Menou (2015) in predicting no limit cycles for present-day Earth, but our results differ toward the outer edge of the HZ. At $S/S_0 = 0.7$, our model predicts stable warm climates above the freezing point, whereas Menou (2015) predicts limit cycles with prolonged glacial conditions. Further outward in the HZ at $S/S_0 = 0.43$ (the effective solar flux at Mars’ orbit), our model and Menou (2015) both predict that the intersection between the weathering rate curve and the greenhouse effect curve falls beneath the freezing point, suggesting that limit cycles should occur. However, when we assume a value of $\beta = 0.3$ in our model, limit cycles do not occur at all (Fig. 1, dashed green curve). Elsewhere (Batalha et al. submitted), we have argued that limit cycles are even more likely to have occurred on early Mars when the solar flux was significantly lower than today. For early Mars, though, the greenhouse effect must be supplemented by some absorber other than H_2O or CO_2 ; otherwise, even brief recoveries to above-freezing surface temperatures are impossible without outside stimuli, e.g., impact events (Segura et al. 2002).

The primary difference between the results of our model and those of Menou (2015) is

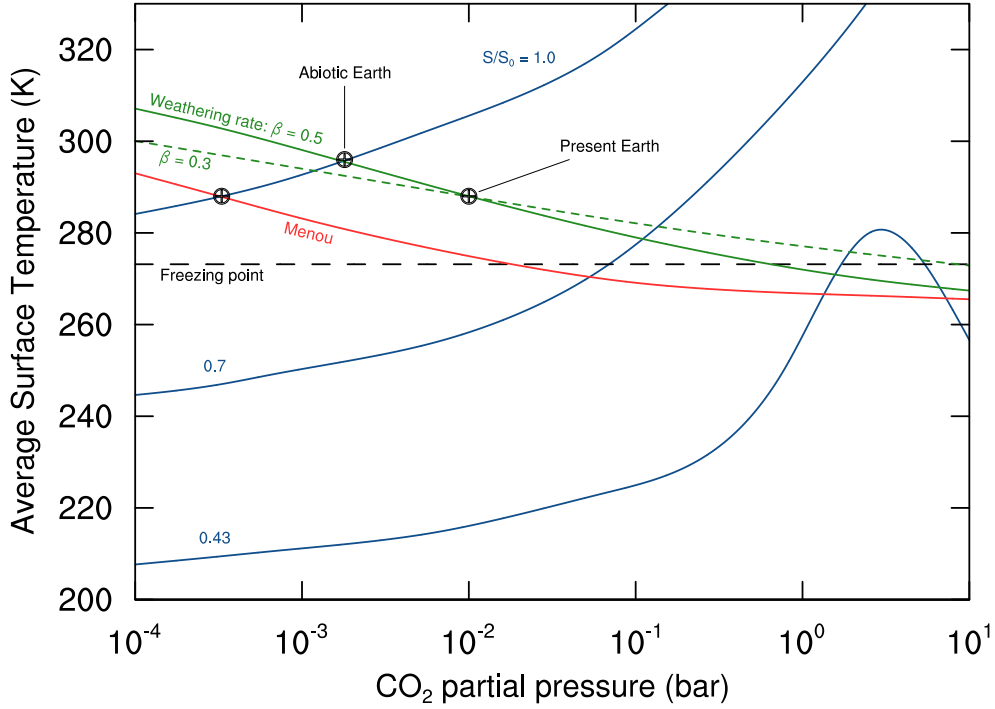


Fig. 1.— Climate calculations indicate where limit cycling should occur. Average surface temperature as a function of $p\text{CO}_2$ (blue curves) is shown for $S/S_0 = 1.0$ (present-day Earth), 0.7 (early Earth), and 0.43 (present-day Mars). Weathering rate curves indicate a model tuned to atmospheric $p\text{CO}_2 = 3.3 \times 10^{-4}$ bar as assumed by (Menou 2015) (red curve) and soil $p\text{CO}_2 = 10^{-2}$ bar as we argue in this study (green curves). Warm stable solutions occur where climate calculations intersect the weathering rate curve above the freezing point, when outgassing and weathering of CO_2 reach a steady-state. For the present-day value of solar flux ($S/S_0 = 1.0$), this intersection indicates the average surface temperature for an abiotic Earth. Note that our estimate of the abiotic Earth temperature is higher than predicted by Menou (2015) because we have tuned our model to present-day soil $p\text{CO}_2$. Limit cycling occurs where climate calculations intersect the weathering rate below the freezing point, when CO_2 accumulates until deglaciation and the onset of weathering.

caused by our higher assumed volcanic outgassing rate and by our treatment of the CO_2 partial pressure of in soil. The relevance of these factors in determining the frequency of limit cycle events is shown in Fig. 2, which shows the limit cycle frequency (in units of cycles per Gyr) as a function of V and p_{\oplus} . The grey region of this figure represents warm, stable solutions that are not prone to limit cycling. When we select $V = 0.1V_{\oplus}$ and $p_{\oplus} = 3.3 \times 10^{-4}$ bar following Menou (2015), Fig. 2 predicts that limit cycles should occur with a frequency of about ten cycles per Gyr. Even if we assume values similar to those used by Kadoya & Tajika (2014), with $V = V_{\oplus}$ and $p_{\oplus} = 3.3 \times 10^{-4}$ bar, this still results in climates prone to limit cycling. However, when we select our preferred values of $V = V_{\oplus}$ as the present volcanic outgassing rate and $p_{\oplus} = 10^{-2}$ bar as the present-day value of $p\text{CO}_2$ in soil, then Fig. 2 predicts that limit cycles should not occur. Our improvements to the radiative transfer and our consideration of the mass balance of CO_2 ice, which was absent in previous studies, make our model more accurate in predicting the frequency of limit cycle events; however, our assumptions about V and p_{\oplus} determine when these limit cycles occur.

When we use our model to investigate the possibility of limit cycles occurring within the Sun’s HZ, we find that no such limit cycle boundary exists for our choices of volcanic outgassing rate ($V_{\oplus} = 70$ bar/Gyr) and soil $p\text{CO}_2$ ($p_{\oplus} = 10^{-2}$ bar). This model configuration allows an Earth-like planet to deglaciate from a snowball state at any point within the conventional HZ due to the accumulation of a dense CO_2 atmosphere from the carbonate-silicate cycle. This result may initially appear inconsistent with Fig. 1, where we predict limit cycles for $S/S_0 = 0.43$. However, the climate calculations in Fig. 1 are global averages from a one-dimensional model (Kopparapu et al. 2013, 2014), in which the surface must be either completely ice-free or completely ice-covered. By contrast, our calculations with a latitudinal EBM in Fig. 3 allow polar ice caps to form while still retaining ice-free conditions at lower latitudes, which permits stable climates to persist across the entire HZ. This illustrates the importance of using latitudinally-resolved models for situations where a planet’s surface is partly ice-covered but remains otherwise habitable. Thus, we still retain a classic picture of the HZ, where warm stable climates (even for abiotic planets) are possible all the way out to the maximum greenhouse effect. This lack of limit cycling throughout the HZ applies to planets orbiting F, G, K, and M stars, as the tuning of our model to soil $p\text{CO}_2$ results in warm stable climates regardless of stellar type. A decrease in β would cause the weathering rate to be even less sensitive to changes in $p\text{CO}_2$, which only expands the climatically stable parameter space where limit cycles do not occur. This suggests that the effect of limit cycling for planets orbiting near the outer edge of the HZ may have been overestimated by previous studies (Kadoya & Tajika 2014, 2015; Menou 2015).

We have argued that volcanic outgassing should balance weathering at the soil $p\text{CO}_2$, rather than the atmospheric $p\text{CO}_2$, which results in no limit cycles for Earth-like planets in

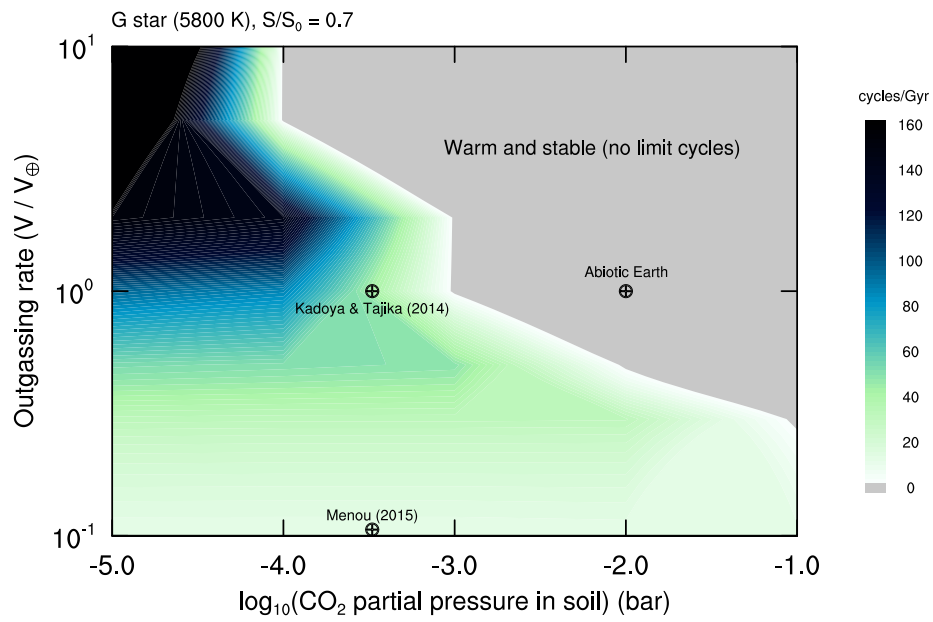


Fig. 2.— Limit cycling is a function of outgassing rate and the partial pressure of CO_2 in soil. The limit cycle frequency is shown for a G star at $S/S_0 = 0.7$, with the grey region illustrating the region of parameter space where limit cycles do not occur. The point labeled ‘Abiotic Earth’ represents our preferred choice of parameters for uninhabited terrestrial planets.

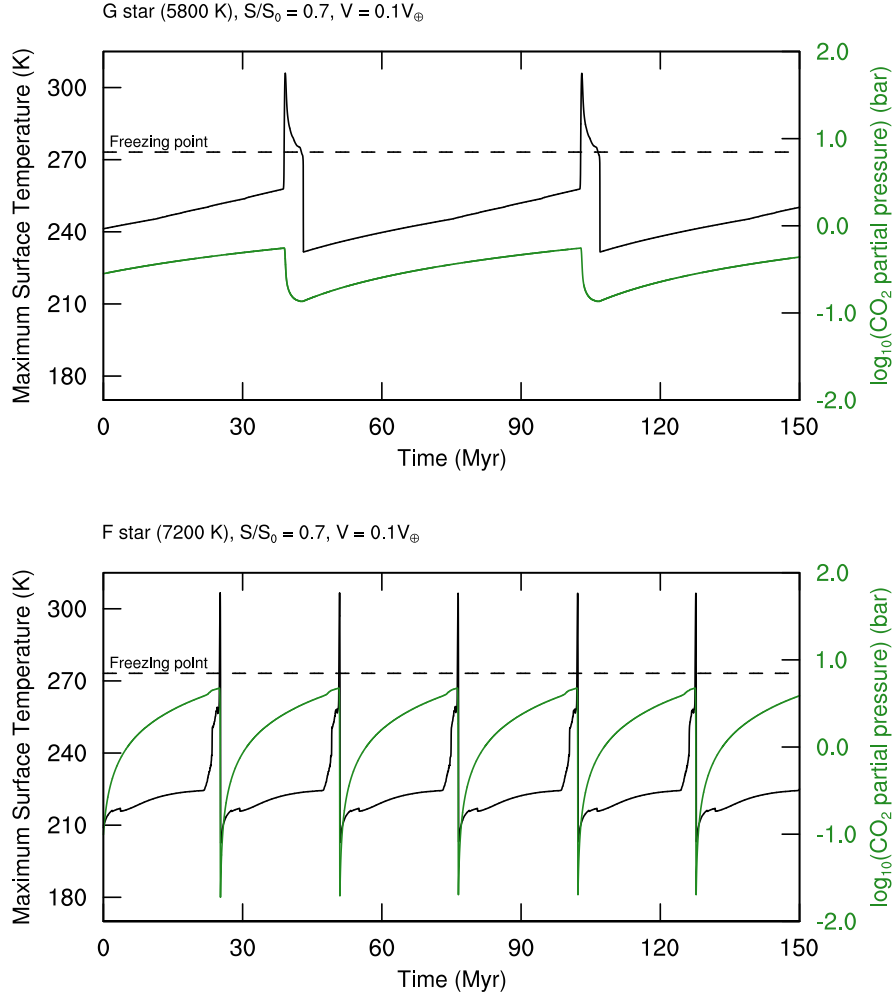


Fig. 3.— Maximum surface temperature (black curve, left axis) and $p\text{CO}_2$ (green curve, right axis) as a function of time for an Earth-like planet with $V = 0.1V_{\oplus}$ orbiting a G star (top panel) and F star (bottom panel) at $S/S_0 = 0.7$. Transient periods of warming during which temperatures exceed the freezing point of water (dashed line) are followed by extended periods of global glaciation. Earth-like planets that exhibit this type of limit cycle cannot maintain permanent surface liquid water and are therefore inhospitable to complex life.

the HZ. However, this result also depends on our assumed volcanic outgassing rate, which we have tuned to present-day Earth. Kadoya & Tajika (2014, 2015) have argued convincingly that the habitability of an Earth-like planet is highly sensitive to the CO₂ degassing rate. (See also earlier papers by Tajika (2003, 2007).) Lower rates of volcanism will decrease atmospheric CO₂, which will increase the susceptibility to limit cycles, as we show in Fig. 2. Furthermore, increased fractional land area could accelerate loss of CO₂ by silicate weathering and make a planet more prone to limit cycles, provided that sufficient rainfall is available. Thus, limit cycles could occur on planets that have a reduced volcanic outgassing rate or increased weathering rate compared to abiotic Earth.

We next consider the effect of volcanic outgassing rate on the occurrence of limit cycles in the HZ. Beginning with a planet orbiting a G-type star, we decrease the volcanic outgassing rate to $V = 0.1V_{\oplus}$, and we calculate the distance at which limit cycles begin by decreasing the relative solar flux S/S_0 until cycles start to develop. (Solar flux and orbital distance are related by the inverse square law.) This transition occurs at $S/S_0 = 0.77$, which corresponds to an orbital distance of about 1.2 AU. At that distance and beyond, the planet’s climate exhibits warm intervals of ~ 5 Myr in duration with equatorial temperatures above the freezing point of water, separated by extended periods of global glaciation lasting ~ 60 Myr (Fig. 3, top panel). During the warm intervals, increased weathering rates lead to a decrease in atmospheric CO₂, which eventually triggers the subsequent glaciation. Because continental weathering ceases entirely during glaciation, atmospheric CO₂ accumulates from ongoing volcanic outgassing.

The effects of limit cycling are quite different for hot, blue, F-type stars than for cooler, red, K- and M-type stars, largely because of the way in which incident stellar radiation interacts with surface water ice. Water ice is highly reflective at visible wavelengths (< 700 nm), but becomes an increasingly efficient absorber at longer, near-infrared wavelengths. Ice-albedo feedback is therefore greater for planets around F stars than it is for planets around K and M stars because F stars emit a greater percentage of their radiation at visible wavelengths (Joshi & Haberle 2012; Shields et al. 2013). For F stars, again assuming $V = 0.1V_{\oplus}$, the limit cycle transition occurs at $S/S_0 = 1.07$, which corresponds to an orbital distance of about 0.96 AU. This planet experiences warm periods lasting ~ 1 Myr with prolonged glacial periods of ~ 20 Myr (Fig. 3, bottom panel). Planets orbiting K- and M-type stars do not experience limit cycles, even at this reduced volcanic outgassing rate, but instead these systems can maintain stable warm conditions all the way out to the maximum greenhouse limit.

Seafloor weathering (Coogan & Gillis 2013) is another potential sink for atmospheric CO₂, which can make a planet more susceptible to limit cycles or permanent glaciation. For a G star planet with $S/S_0 = 0.7$ and $V = 0.1V_{\oplus}$ that is already experiencing limit cycles,

an increase in the rate of seafloor weathering serves to decrease the frequency in cycles between climate states, which results in longer extended periods of glaciation between warm episodes (Fig. 4). The rate of seafloor weathering may also be sensitive to atmospheric $p\text{CO}_2$ through the parameter γ in Eq. (4), but increases in γ only accentuate the tendency of a planet in a limit cycle toward permanent glaciation. For planets beyond the limit cycle region, an increase in seafloor weathering will cause the limit cycle region of the HZ to expand, analogous to a decrease in volcanic outgassing of the same magnitude. The rest of our calculations will consider sensitivity to the volcanic outgassing rate, V , but these results apply more broadly to the difference between volcanic outgassing and seafloor weathering, $V - W$, that drives long-term changes in $p\text{CO}_2$ (Eq. (3)). Strong seafloor weathering could cause a planet to be prone to limit cycles even if the volcanic outgassing rate is at or above present-day values.

We summarize our findings by performing similar calculations of the limit cycle boundary for F, G, K, and M stars with $V = 0.5V_{\oplus}$ and combining these calculations with the results for $V = 0.1V_{\oplus}$ in Fig. 5. As discussed above, planets with a present-day volcanic outgassing rate avoid limit cycling altogether, while a rate of $V = 0.5V_{\oplus}$ or lower can be sufficient to induce cycling for at least part of the HZ. Planets orbiting F stars exhibit cycling behavior throughout a large region of their HZs and are the most responsive to changes in V , as a result of their increased sensitivity to ice-albedo feedback. A planet like Earth around a G star should have experienced limit cycles in its past only if volcanic outgassing were much lower than today. Modern Earth avoids this fate, but early Earth may have experienced repeated Snowball Earth episodes if volcanic outgassing rates were relatively low (Sleep & Zahnle 2001; Tajika 2007). The rock record is sparse or nonexistent during the first half of Earth’s history, so such behavior could have occurred but remained undetected.

By contrast, late K and M star planets can maintain stable climates without cycling until the maximum greenhouse limit is reached. Such planets are subject to tidal locking and may show only one face to the star, as the Moon does to Earth, which may or may not present a problem for complex life. However, planets orbiting these stars may lose their entire water inventory as a consequence of a runaway greenhouse during the extended, hot pre-main sequence evolution of the host star (Ramirez & Kaltenegger 2014; Luger & Barnes 2015; Tian & Ida 2015). This suggests that such planets may be entirely uninhabitable unless they begin with an abundant water inventory or water is somehow resupplied after the star enters the main sequence.

Note that the HZ itself is also narrower in Fig. 5 than prior estimates because the requirement for a planet to be able to recover from global glaciation shifts the outer edge slightly inward in our model. This last result is sensitive to the fraction of the planet’s

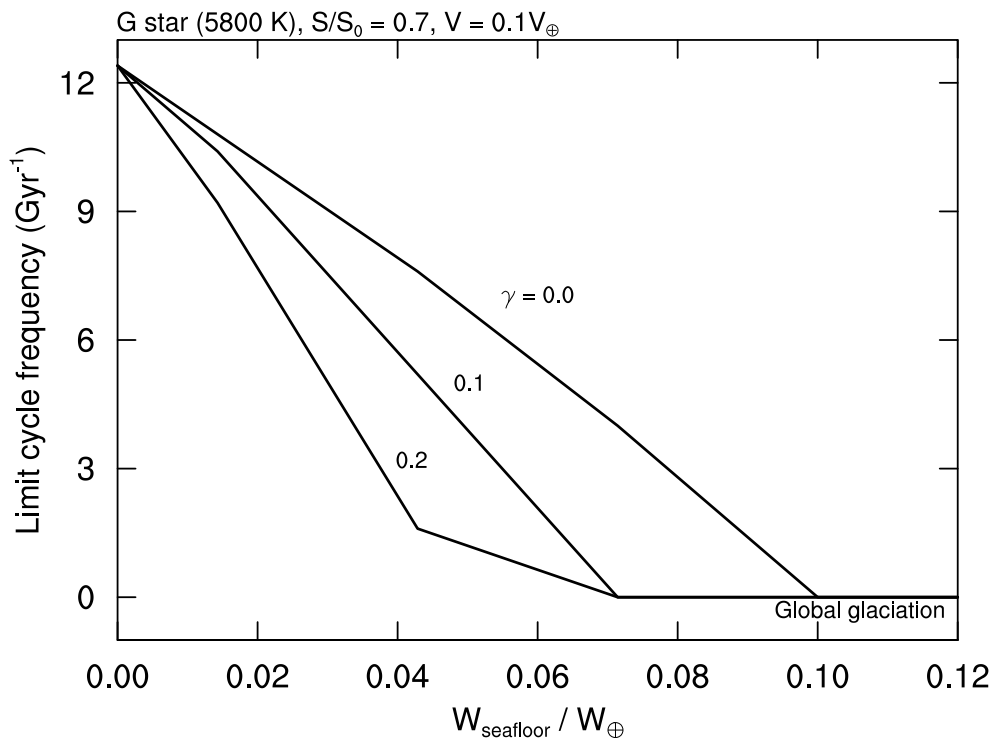


Fig. 4.— Diagram showing the dependence of the limit cycle frequency on seafloor weathering rate for an Earth-like planet with $V = 0.1V_{\oplus}$ orbiting a G star at $S/S_0 = 0.7$, with sensitivity to the seafloor weathering parameter γ . Complete decoupling of $p\text{CO}_2$ from seafloor weathering ($\gamma = 0$) results in a steady decline in the frequency of limit cycle warming events as the seafloor weathering rate increases, until the uptake of CO_2 by the seafloor equals the outgassing rate. When the rate seafloor weathering depends on $p\text{CO}_2$ ($\gamma > 0$), then the accumulation of CO_2 in the atmosphere from outgassing drives stronger seafloor weathering and makes the planet more prone to permanent glaciation.

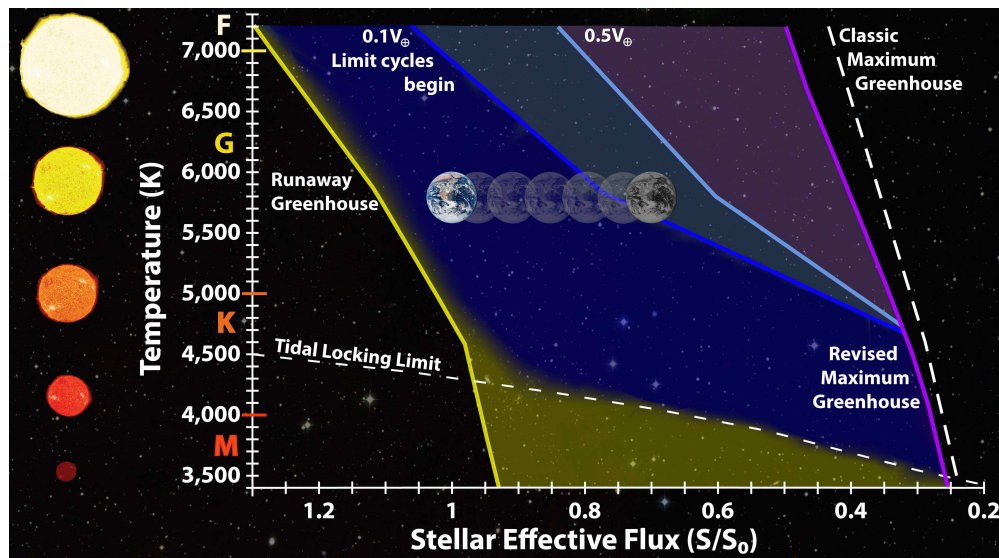


Fig. 5.— Habitable zone boundaries for various stellar types as a function of stellar effective flux, normalized to that at Earth’s orbit today (S_0). The ‘runaway greenhouse’ and ‘classic maximum greenhouse’ limits (solid blue curves) show the conventional HZ boundaries (Kopparapu et al. 2013), as corrected to account for recent 3-D studies (Leconte et al. 2013). The ‘revised maximum greenhouse’ limit (dashed blue curve) shows the flux beyond which an Earth-like planet would be unable to deglaciate from an initial snowball state. (The classic maximum greenhouse assumes an ice-free surface, which is inconsistent with the limit cycle behavior described here.) Planets beyond this boundary are thus uninhabitable at their surfaces. The boundaries labeled ‘Limit cycles begin’ marks the region beyond which a stable warm climate cannot be maintained for volcanic outgassing rates in the range $0.1V_{\oplus} < V < 0.5V_{\oplus}$. Modern Earth is shown, along with Earth at 4.5 Gyr ago, when the solar flux was ~ 70 percent of its current value.

surface covered by (lower albedo) bare ice, as opposed to (higher albedo) snow-covered ice. In our model the ice is snow-covered at all latitudes, and so its albedo remains relatively high, even in the near-infrared. By contrast, Shields et al. (2013) found that the outer edge should be completely insensitive to surface albedo because its effect would be completely masked by the overlying dense CO₂-rich atmosphere. However, such dense CO₂ atmospheres may not be long-lived when carbonate-silicate weathering is included.

4. Discussion

The Rare Earth hypothesis (Ward & Brownlee 1999) suggests that complex life may be uncommon in the universe even if simple life is widespread. Although many arguments have been raised against this idea (Kasting 2001), limit cycling in parts of the conventional HZ, for planets with relatively low outgassing rates, presents problems for both simple and complex life. Photosynthetic algae and cyanobacteria would go extinct on a ‘hard Snowball’ planet with sea-ice thicknesses of a kilometer or more, unless illuminated refugia were available. Both types of organisms survived the Neoproterozoic Snowball Earth episodes (Hoffman et al. 1998), so some types of refugia must have existed. Models with either thin ice (Pollard & Kasting 2005) or open water (Abbot et al. 2011) near the equator may provide the explanation. But multicellular land life would be highly challenged by this type of climatic behavior which, fortunately, has not occurred since the late Precambrian. It follows that animal life, and thus intelligent life, may not be able to evolve on planets with low incident stellar flux and a low volcanic outgassing rate, even if they are within the conventional HZ.

The presence of a limit cycle boundary depends critically upon the assumed volcanic outgassing rate, and planets with a CO₂ outgassing rate similar to today may not experience limit cycles at all. Kadoya & Tajika (2015) suggest that low outgassing rates may be expected for Earth-like planets orbiting old stars, which would make such planets more prone to limit cycles. One should exercise caution in accepting this conclusion, as it is based on their assumption that the CO₂ outgassing rate declines monotonically with time on an Earth-like planet as its interior cools. Other authors (Holland 2009) have suggested that Earth’s CO₂ outgassing rate actually *increased* with time during the first half of its history as the growth of continents allowed greater storage of carbonate rocks and greater recycling of CO₂ through weathering, carbonate deposition, and sediment subduction.

If the CO₂ outgassing rate of present-day Earth is anomalously large compared to typical terrestrial planets, then Earth might be uncommon in its ability to sustain a stable warm climate. Conversely, planets more massive than Earth (known as super-Earths) may exhibit

higher rates of volcanism than Earth today, although the dependence of plate tectonics on planetary mass remains unclear (Valencia et al. 2007; Kite et al. 2009; Korenaga 2010; van Heck & Tackley 2011; Haghighipour 2013). So, it is at least conceivable that super-Earths in the outer parts of the HZ would be better abodes for complex life than would true Earth analogs.

The actual dependence of the silicate weathering rate on $p\text{CO}_2$ is unknown for abiotic planets. We have assumed $\beta = 0.5$, which matches the behavior of the H^+ concentration in rainwater; however, the actual exponent could range from 0.25 to 1 (Berner 1994). The weathering rate on modern Earth is sometimes argued to have zero direct dependence on atmospheric CO_2 (Berner et al. 1983), because $p\text{CO}_2$ in soils is decoupled from atmospheric $p\text{CO}_2$ by the presence of vascular plants, which pump up soil CO_2 by way of root respiration. Plants also generate humic acids which accelerate weathering, again without any direct relation to atmospheric $p\text{CO}_2$. Consequently, Menou (2015) argued that the emergence of land life on a planet should stabilize its climate against limit cycles. But this inference is incorrect. Land plants accelerate weathering (Berner 1992) by anywhere from a factor of 2-3 (Cawley et al. 1969) to a factor of 10-100 or more (Schwartzman & Volk 1989) compared to an abiotic environment. (We assume a weathering acceleration factor in the range of 2.8-5.5, as discussed above.) Lichens, algae, and other microorganisms also secrete acids that accelerate weathering (Berner 1992), so the emergence of life on a planet in the outer, limit-cycling region of the HZ should only help to pull down atmospheric CO_2 , making the planet even more subject to global glaciation. Global glaciation would kill any plants, allowing atmospheric CO_2 to again accumulate, and so cycling should re-initiate at a rate that would depend on whether the plants themselves were able to regenerate. Life (as we know it) would not stabilize a planet’s climate against limit cycling, but it might create a more complex, biologically mediated form of limit cycling.

What do these arguments imply about the prevalence of animal life and the possible evolution of intelligent life? The limit cycle region of the HZ depends upon the assumed, and somewhat uncertain, behavior of the volcanic outgassing and seafloor weathering rates for abiotic planets. For planets around K and M stars, this does not appear to pose a problem, but for some types of stars, the outlook is less optimistic. According to our results in Fig. 5, the HZ around F stars can be nearly eliminated if the volcanic outgassing rate is $0.1V_{\oplus}$ or less. F stars also have relatively short main sequence lifetimes, and they brighten quickly as they age, which limits the time available for biological evolution. Meanwhile, although planets around K and M stars may avoid this problem, they may have other issues that could preclude their habitability. If Ramirez & Kaltenegger (2014), Luger & Barnes (2015), and Tian & Ida (2015) are correct, nearly all planets around late K and M stars should experience drastic pre-main-sequence water loss. Early K stars and late G stars avoid both

of these problems. So, there are still many stars that could host planets with complex life. But any search for such life should be concentrated on planets around late G- to early K-type stars, which are only a subset of the planets that might support simple life.

5. Conclusion

We have calculated the limit cycle boundary of the habitable zone as a function of stellar type and CO_2 outgassing rate. Earth-like planets with volcanic outgassing rates similar to today are able to maintain stable climates across the entire range of the HZ, regardless of stellar type. But planets with lower volcanic outgassing rates or significant seafloor weathering rates should experience limit cycles, with punctuated episodes of warm conditions followed by extended glacial periods. F star planets are the most prone to this behavior as a result of increased susceptibility to ice-albedo feedback. Planets orbiting late K and M stars avoid limit cycles because of reduced ice-albedo feedback, but they may suffer from water loss during their formation. Thus, systems with the greatest potential for habitability are those around late G and early K type stars.

The net outgassing rate of CO_2 and partial pressure of CO_2 in soil are key parameters in understanding the habitability of an Earth-like planet. If Earth has maintained a net CO_2 outgassing rate at or above its current value for its entire history, then it may never have been prone to limit cycles at any point in time. By extension, if Earth's outgassing rate is typical for other terrestrial planets, then limit cycles may not pose a problem for habitability at all. Likewise, we expect that an abiotic planet would accumulate more atmospheric CO_2 than its inhabited counterpart, which would lead us to expect that few planets, if any, should reside in limit cycles. However, we should expect a diversity of exoplanet environments to exist, and we cannot rule out the possibility that Earth's CO_2 inventory is atypical. In the search for habitable worlds, we should at least consider the possibility that some Earth-like planets may exhibit lower net outgassing rates than today, which could develop limit cycles and preclude the development of complex life.

The authors thank Darren Williams for assistance with model development as well as Dorian Abbot, Ray Pierrehumbert, Aomawa Shields, and Russell Deitrick for helpful discussions. The authors also thank an anonymous reviewer for thoughtful comments which greatly improved the manuscript. J.H. acknowledges funding from the NASA Habitable Worlds program under award NNX15AQ82G. R.K.K. and J.F.K. acknowledge funding from NASA Astrobiology Institute's Virtual Planetary Laboratory lead team, supported by NASA under cooperative agreement NNH05ZDA001C. R.K.K. and J.H. also acknowledge funding from

the NASA Habitable Worlds program under award NNX16AB61G. This material is based upon work supported by the National Science Foundation under Grant No. DGE1255832 to N.E.B. Any opinions, findings, and conclusions or recommendations expressed in this material are those of the authors and do not necessarily reflect the views of NASA or the National Science Foundation.

A. Polynomial fits to OLR and planetary albedo for F, G, K, and M stars

We parameterized top of the atmosphere (TOA) albedo, α , and the outgoing IR flux, F_{OLR} , as polynomials with the following variables: surface temperature T_s (K) used as $t = \log_{10}(T_s)$; $\phi = \log_{10}(p\text{CO}_2)$, where $p\text{CO}_2$ is the partial pressure of CO_2 (bars); $\mu = \cos(z)$ where z is the zenith angle; and surface albedo a_s . The parameterizations were derived by running a 1-D radiative convective (RC) model (Kopparapu et al. 2013, 2014) over a range of values of the above parameters with a 1 bar N_2 noncondensable background for each stellar type. The fits are valid in the range $150 \text{ K} < T_s < 350 \text{ K}$, $10^{-5} \text{ bar} < p\text{CO}_2 < 35 \text{ bar}$, $0.2 < a_s < 1$ and $0 < \mu < 1$. For planetary albedo, we made separate fits above and below 250 K.

Solar zenith angle is explicitly calculated at each latitude in the EBM as a function of solar declination and solar hour angle, averaging over a complete rotation to obtain the insolation-weighted zenith angle (Williams & Kasting 1997; Cronin 2014). In general, we expect that TOA should increase as a function of z . The usual configuration of our 1-D RC model (Kasting 1991; Kasting et al. 1993; Kopparapu et al. 2013, 2014) assumes that stratospheric temperature T_{strat} is equal to the ‘skin temperature’ of a gray atmosphere (i.e., the temperature at an optical depth of zero), given by

$$T_{strat} = \frac{1}{2^{1/4}} \left[\frac{S}{4\sigma} (1 - \alpha) \right], \quad (\text{A1})$$

where σ is the Stefan-Boltzmann constant. However, Eq. (A1) is only appropriate for global average conditions (i.e., for $z = 60^\circ$) and cannot be applied to calculate T_{strat} and α for the range of solar zenith angles across all latitude bands represented in our EBM. In order to circumvent this problem, we followed Williams & Kasting (1997) and parameterized T_{strat} as a function of z :

$$T_{strat}(Z) = T_{strat}(60^\circ) \left[\frac{F_s(z)}{F_s(60^\circ)} \right]^{1/4}, \quad (\text{A2})$$

where F_s is the absorbed fraction of incident solar flux, which was calculated for a variety of zenith angles between 0° and 90° using the radiative-convective model. The value of

$T_{\text{strat}}(60^\circ)$ was obtained using Eq. (A1) above. This configuration of our RC model allows the parameterizations of TOA below to accurately decrease with z as expected.

A.1. Parametric expressions for OLR and Planetary Albedo

The coefficients are provided as downloadable ASCII data tables in online supplementary information. The rows in the data table correspond to the order of the coefficients in the following expressions. The OLR coefficients are the same for all different stars, as it is a planet specific property and variation in stellar type does not change it. For planetary albedo coefficients, each stellar type has two sets of data tables, one for surface temperatures between 150 K to 250 K and another for 250 K to 350 K.

$$F_{OLR} = At^4 + Bt^3\phi + Ct^3 + Dt^2\phi^2 + Et^2\phi + Ft^2 + Gt\phi^3 + Ht\phi^2 + It\phi + Jt + K\phi^4 + L\phi^3 + M\phi^2 + N\phi + \text{constant1} \quad (\text{A3})$$

$$\begin{aligned} \alpha(t, a_s, \mu, \phi) = & A\mu^3 + B\mu^2a_s + C\mu^2t + D\mu^2\phi + E\mu^2 + F\mu a_s^2 + G\mu a_s t + H\mu a_s \phi + I\mu a_s \\ & + J\mu t^2 + K\mu t\phi + L\mu t + M\mu\phi^2 + N\mu\phi + O\mu + Pa_s^3 + Qa_s^2t + Ra_s^2\phi + Sa_s^2 \\ & + Ta_s t^2 + Ua_s t\phi + Va_s t + Wa_s\phi^2 + Xa_s\phi + Ya_s + Zt^3 + AAt^2\phi + ABt^2 \\ & + ACt\phi^2 + ADt\phi + AEt + AF\phi^3 + AG\phi^2 + AH\phi + \text{constant2} \end{aligned} \quad (\text{A4})$$

These parametric fits provide a rapid means of obtaining OLR and planetary albedo from our 1-D RC climate model calculations. The error between the climate model data and the parametric fits for OLR does not exceed 2%, and the error distributions of planetary albedo for different stellar spectral types show that a majority of parametric fits have less than 20% uncertainty. Error plots for OLR and planetary albedo are provided as online supplementary information.

REFERENCES

- Abbot, D., Voigt, A., & Koll, D. 2011, *J. Geophys. Res.*, 116, D18103
- Abbot, D. S., Cowan, N. B., & Ciesla, F. J. 2012, *ApJ*, 756, 178
- Abe, Y., Abe-Ouchi, A., Sleep, N. H., & Zahnle, K. J. 2011, *Astrobiol.*, 11, 443
- Allard, F., Allard, N. F., Homeier, D., et al., 2007, *A&A*, 474, L21-L24

- Batalha, N. E., Kopparapu, R. K., Haqq-Misra, J., & Kasting, J. F., submitted, *Earth Planet. Sci. Lett.*
- Berner, R. A., Lasaga, A. C., & Garrels, R. M. 1983, *Am. J. Sci.*, 283, 641
- Berner, R. A., 1992, *Geochim. Cosmochim. Acta*, 56, 3225
- Berner, R. A., 1994, *Am. J. Sci.*, 294, 56
- Berner, R. A. & Kothavala, Z., 2001, *Am. J. Sci.*, 301, 182
- Cawley, J. L., Burruss, R. C., Holland, H. D., 1969, *Science*, 165, 391
- Colaprete, A. & Toon, O. B., 2003, *J. Geophys. Res.*, 108, 5025
- Coogan, L. A. & Gillis, K. M., 2013, *Geochem. Geophys. Geosys.*, 14, 1771
- Cronin, T. W., 2014, *J. Atmos. Sci.*, 71, 2994
- Fairén, A. G., Haqq-Misra, J. D., & McKay, C. P. 2012, *A&A*, 540, A13
- Forgan, D., 2013, *MNRAS*, 437, 1352
- Forget, F. & Pierrehumbert, R., 1997, *Science*, 278, 1273
- Forget, F., Wordsworth, R., Millour, E., et al., 2013, *Icarus*, 222, 81
- Gaidos, E. & Williams, D. M., 2004, *New Astron.*, 10, 67
- Gerlach, T., 2011, *Eos*, 92, 201
- Haghighipour, N., 2013, *Annu. Rev. Earth Planet. Sci.*, 41, 469
- Haqq-Misra, J., 2014, *J. Adv. Model. Earth Syst.*, 6, 950
- Holland, H. D., 2009, *Geochim. Cosmochim. Acta* 73, 5241
- Hoffman, P. F., Kaufman, A. J., Kalverson, G. P., & Schrag, D. P., 1998, *Science*, 281, 1342
- Jarrard, R. D., 2003, *Geochem. Geophys. Geosyst.*, 4, 8905
- Joshi, M. M. & Haberle, R. M., 2012, *Astrobiol.*, 12, 3
- Kadoya, S. & Tajika, E., 2014, *ApJ*, 790, 107
- Kadoya, S. & Tajika, E., 2015, *ApJ*, 815, L7

- Kaltenegger, L. & Sasselov, D., 2011, *ApJ*, 736, L25
- Kane, S. R. & Gelino, D. M., 2012, *Astrobiol.*, 12, 940
- Kane, S. R. & Hinkel, N. R., 2013, *ApJ*, 762, 7
- Kasting, J., 1991, *Icarus*, 94, 1
- Kasting, J., 2001, *Persp. Biol. Med.*, 44, 117
- Kasting, J. F., Whitmire, D. P., & Reynolds, R. T. 1993, *Icarus*, 101, 108
- Kite, E. S., Manga, M., & Gaidos, E., *ApJ*, 700, 1732
- Kitzmann, D., 2016, *ApJ*, 817, L18
- Kopparapu, R. K., Ramirez, R., Kasting, J. F., et al., 2013, *ApJ*, 765, 131
- Kopparapu, R. K., Ramirez, R., SchottelKotte, J., et al., 2014, *ApJ*, 787, L29
- Korenaga, J., 2010, *ApJ*, 725, L43
- Kravchenko, Y. & Krupskii, I., 1986, *Sov. J. Low Temp. Phys*, 12, 46
- Kump, L. R., Brantley, S. L., & Arthur, M. A. 2000, *Annu. Rev. Earth Planet. Sci.*, 28, 611
- Kump, L. R., Kasting, J. F., & Crane, R. G. 2010, *The Earth System*, Upper Saddle River, NJ
- Lagache, M., 1976, *Geochim. Cosmochim. Acta*, 40, 157
- Lecante, J., Forget, F., Charnay, B., et al., 2013, *A&A*, 554, A69
- Luger, R. & Barnes, R., 2015, *Astrobiol.*, 15, 119
- Menou, K., 2015, *Earth Planet. Sci. Lett.*, 429, 20
- Mills, B., Watson, A. J., Goldblatt, C., et al., 2011, *Nat. Geosci.*, 4, 861
- Mischna, M. A., Kasting, J. F., Pavlov, A., & Freedman, R., 2000, *Icarus*, 145, 546
- North, G. R., Cahalan, R. F., & Coakley, J. A. 1981, *Rev. Geophys.*, 19, 91
- Pavlov, A. A., Hurtgen, M. T., Kasting, J. F., & Arthur, M. A., 2003, *Geology*, 31, 87
- Pollard, D. & Kasting, J. F., 2005, *J. Geophys. Res.*, 110, C07010

- Ramirez, R. & Kaltenegger, L., 2014, *ApJ*, 797, L25
- Rothman, L. S., Gordon, I. E., Barbe, A., et al., 2009, *J. Quant. Spectrosc. Radiat. Transfer*, 110, 533
- Rothman, L. S., Gordon, I. E., Barbe, A., et al., 2010, *J. Quant. Spectrosc. Radiat. Transfer*, 111, 2139
- Saal, A. E., Hauri, E. H., Langmuir, C. H., & Perfit, M. R., 2002, *Nature*, 419, 419
- Schwartzman, D. W. & Volk, T., 1989, *Nature*, 340, 457
- Segura, T. L., Toon, O. B., Colaprete, A., Zahnle, K., 2002, *Science* 298, 1977
- Shields, A. L., Meadows, V. S., Bitz, C. M., et al., 2013, *Astrobiol.*, 13, 715
- Showman, A. P., Wordsworth, R. D., Merlis, T. M., et al., 2013, *Comparative Climatology of Terrestrial Planets*, 277
- Sleep, N. H. & Zahnle, K., 2001, *J. Geophys. Res.*, 106, 1373
- Stewart, S. T. & Nimmo, F., 2002, *J. Geophys. Res.*, 107, 5069
- Tajika, E., 2003, *Earth Planet. Sci. Lett.*, 214, 443
- Tajika, E., 2007, *Earth Planet. Space*, 59, 293
- Tian, F. & Ida, S., 2015, *Nat. Geosci.*, 8, 177
- Valencia, D., O’Connell, R. J., & Sasselov, D. D., *ApJ*, 670, L45
- van Heck, H. J. & Tackley, P. J., 2011, *Earth Planet. Sci. Lett.*, 310, 252
- Vladilo, G., Murante, G., Silva, L., et al., 2013, *ApJ*, 767, 65
- von Braun, K., Boyajian, T. S., Kane, S. R., et al., 2011, *ApJ*, 729, L26
- Walker, J. C. G., Hays, P. B., & Kasting, J. F., *J. Geophys. Res.*, 86, 9776
- Ward, P. D. & Brownlee, D., 1999, *Rare Earth*, Springer-Verlag, New York
- Warren, S. G., Wiscombe, W. J., & Firestone, J. F. 1999, *J. Geophys. Res.*, 95, 14717
- Williams, G. P. & Halloway, J., 1982, *Nature*, 297, 295
- Williams, D. M. & Kasting, J. F., 1997, *Icarus*, 129, 254

Wolf, E. T. & Toon, O. B., 2014, *Geophys. Res. Lett.*, 41, 167

Yang, J., Boué, G., Fabrycky, D. C., & Abbot, D. S., 2014, *ApJ*, 787, L2